

Numerical Study of Triple-Shock-Wave Structure in Steady Irregular Reflection

G.V. Shoev, D.V. Khotyanovsky, Ye.A. Bondar,
A.N. Kudryavtsev and M.S. Ivanov

*Khristianovich Institute of Theoretical and Applied Mechanics, Institutskaya 4/1, Novosibirsk,
Russia, 630090*

Abstract. The viscosity effects on strong and weak shock wave reflection are investigated with the Navier-Stokes and DSMC flow solvers. It is shown that the viscosity plays a crucial role in the vicinity of three-shock intersection. Instead of a singular triple point, in viscous flow there is a smooth three shock transition zone, where one-dimensional shock jump relations cannot be applied. At the flow parameters corresponding to the von Neumann reflection, when no inviscid three-shock solution exists, the computations predict an irregular shock-wave configuration similar to that observed previously in experiments. The existence of a viscous zone in the region of shock-wave interaction allows a continuous transition from the parameters behind the Mach stem to the parameters behind the reflected shock, which is impossible in the inviscid three-shock theory.

Keywords: von Neumann paradox, irregular shock wave reflection.

PACS: 47.40.Ki, 47.35.Lf.

INTRODUCTION

Many interesting phenomena that occur in oblique shock wave reflection have been discovered in the past. The main feature herein is the existence of two possible configurations of shocks, regular and irregular. Irregular reflection, which is shown in the figure 1, is shock wave pattern that combines the incident (IS) and reflected (RS) shock waves and the Mach stem (MS).

Classical theoretical methods such as the shock polar analysis and the three-shock theory based on Rankine–Hugoniot jump conditions across oblique shocks were developed by J. von Neumann to describe shock wave configurations. These theoretical methods predict well most of the features of shock wave interaction. However, in reflection of weak shock waves ($M_\infty < 2.2$ in air), there is a range of flow parameters where the von Neumann three-shock theory does not produce any solution, whereas numerous experiments and numerical simulations [1,2] reveal a three-shock structure similar to the Mach reflection pattern. This inconsistency is usually referred to as the von Neumann paradox. One of the possible approaches to resolve the von Neumann paradox is to account for viscous effects in the vicinity of the triple point [3, 4]. Instead of a triple point, in viscous flow there is a smooth region of three-shock wave intersection. Because of the large gradients of the flow parameters and gas nonequilibrium inside the shock waves, the applicability of the Navier–Stokes (NS) equations to describe the flow parameters within three-shock intersection region cannot be taken for granted. Also, because of the characteristic length scale of this zone comparable with the shock wave thickness [3], which is a few dozens of mean free path, it looks like kinetic effects can be important here. It is well known that the kinetic approach based on flow modeling by the Direct Simulation Monte Carlo (DSMC) method [5] ensures an exact description of the internal structure of shock waves. Therefore, it seems essential that the results of the NS computations should be compared with the results obtained by the DSMC method, which can be considered as the method of solving the kinetic Boltzmann equation. Cross comparison of the results is also important because of the lack of the experimental data on the flow structure in the close vicinity of the shock intersection. The basic goal of the present study was a numerical investigation of viscous effects in irregular reflection of strong and weak shock waves.

PROBLEM FORMULATION AND NUMERICAL TECHNIQUES

We studied the reflection of an oblique shock wave with an angle of incidence α generated by a wedge in a steady flow with different Mach number from the plane of symmetry as shown in Fig. 1. A slipstream, that is, a contact discontinuity, emanates from the triple point T (Fig 1a) due to inequality of entropy in the flow passing through the incident and reflected shocks and the flow passing through the Mach shock. The flow behind the Mach shock is subsonic and is gradually accelerated back to supersonic speed owing to influence of expansion waves emanating from the trailing edge of the wedge and transmitted through the reflected shock. As a result, a closed subsonic pocket is formed behind the Mach stem.

The Navier–Stokes code is a time-explicit shock-capturing code based on fifth-order WENO reconstruction [6] of convective terms and a mixed, central-biased, fourth-order approximation of dissipation terms. The computations were run in a rectangular computational domain (see Fig. 1b) with uniform grid spacing. The left boundary of the computational domain is a supersonic inflow with the free stream flow parameters imposed. The right boundary of the domain was placed far enough downstream to ensure supersonic outflow conditions there. Extrapolation of the flow variables was used to impose boundary conditions at the outflow. At the lower boundary of the domain, symmetrical boundary conditions (specular reflection) were used. The upper boundary was placed at $y=g$ corresponding to the vertical position of the trailing edge of the wedge. The boundary conditions on the upper boundary were specified in a complex manner to maintain flow conditions at the horizontal line $y=g$. Supersonic free stream conditions were specified along the segment 1–2 of the upper boundary (see Fig. 1b). The segment 2–3 corresponds to the intersection of the upper boundary with the incident shock, where in the viscous case a smooth variation of the flow parameters inside the shock wave should be specified. For the internal structure of the shock wave we used the analytical solution of the one-dimensional Navier–Stokes equations that can be found in [7]. Along the line segment 3–4 the flow parameters corresponding to Rankine–Hugoniot conditions behind the incident shock were imposed. Along the segment 4–5 the inviscid wall (symmetry) boundary conditions were used. The computations were started with a uniform supersonic flow filling the entire computational domain. The numerical solution was then advanced in time with the second-order Runge–Kutta scheme until a steady state was achieved.

The DSMC simulations are performed with the SMILE code [8], which uses the majorant frequency method for computing collision integrals. The computational domain was similar to the domain used in the Navier–Stokes computations (see Fig. 1b). Separate rectangular grids were used for modeling molecular collisions and sampling the gas dynamic parameters. The first grid was uniform, and its linear size was less than the minimum value of the mean free path in the computational domain. The second grid was condensed in the zones of interest: the Mach stem and the point of the shock reflection from the symmetry plane. At the initial moment, the domain was populated by the model particles according to the Maxwell distribution function corresponding to the free stream parameters. Free stream conditions were imposed on the left boundary and on a portion of the upper boundary of the computational domain. The right (downstream) boundary was selected so that the flow there was supersonic. A specular reflection condition was used at the lower boundary (the symmetry plane), the wedge surface, and the part of the upper boundary ($y=g$). The computations properly resolved the internal structure of the shock waves.

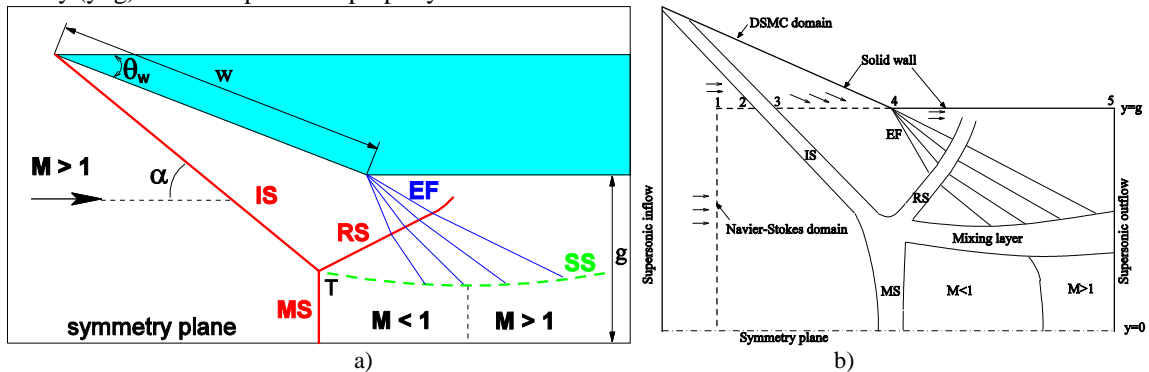


FIGURE 1. a) Schematic of irregular shock wave reflections. b) Schematic of the Navier–Stokes and DSMC computational domains and boundary conditions. IS is incident shock, RS is reflected shock, MS is Mach shock, and EF is expansion fan.

A flow of the monatomic gas argon with a ratio of specific heats $\gamma=5/3$ and a Prandtl number $Pr=0.66$ was considered. We examined two cases: reflection of strong shock waves (Mach number of the free stream $M_\infty=4$ and wedge angle $\Theta_w=25$ deg) and reflection of weak shock waves (Mach number of the free stream $M_\infty=1.7$ and wedge angle $\Theta_w=13.5$ deg); the corresponding inviscid solutions shown are in Fig. 2. In the first case, the three-shock solution marked as MR in Fig. 2a predicts the values of pressure and flow deflection at the triple point $p/p_\infty=19.57$

and $\Theta_w=12.42$ deg, respectively. In the second case, there is no three-shock solution – shock polars do not interest each other (fig. 2b). This case corresponds to von Neumann paradox conditions. Guderley [9] developed a first non-contradictory inviscid theoretical model for weak shock wave reflection that assumed the existence of a Prandtl–Meyer expansion and a local supersonic patch behind the triple point. Developing this theory, Vasil’ev and Kraiko [10] proposed an inviscid solution in the plane (θ, p) , which was an isentrope emanating from the sonic point of the reflected wave polar (figs. 2b and 10b).

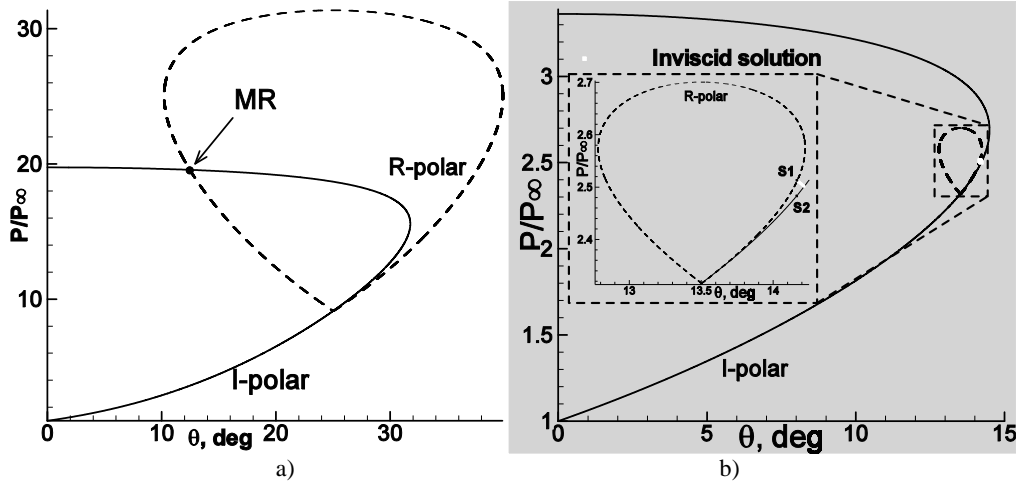


FIGURE 2. Theoretical solutions for irregular reflections in the (θ, p) plane. a) three-shock solution marked as MR; b) sonic points of the incident and reflected shock polars marked as S1 and S2, respectively.

RESULTS AND DISCUSSION

The DSMC and NS computations for $M_\infty=4$ at different Knudsen numbers are compared in the Fig. 3. It is seen that the DSMC and NS results (both the shock wave width and the Mach stem height and coordinate) are substantially different at the Knudsen numbers $Kn=0.01$ and 0.003 . Beginning from the Knudsen number $Kn=0.001$, the NS computation agrees well with the DSMC computation.

For a detailed comparison of the triple-shock structure, Fig. 4 shows the pressure profiles for the NS and DSMC computations, as compared with the value predicted by the three-shock theory. The pressure profiles are constructed at a constant Y coordinate, so that the profiles pass through the center of the triple-shock structure. It is seen from the figure that the NS triple-shock wave is steeper and narrower than the corresponding DSMC predictions. In both cases, however, the pressure finally reaches the same value, despite the difference in the shock profiles of the triple-shock structure. The maximum pressure is greater than the pressure predicted by the three-shock theory by $\sim 10\%$ for the DSMC calculation and the Navier–Stokes equations.

A detailed comparison of the numerical results with the theoretical predictions is given in Fig. 5, where the values of pressure and flow deflection angle θ extracted from the numerical flow fields immediately behind the Mach stem and the reflected shock are plotted against the analytical shock polar solution in the (θ, p) plane. The values were taken along the contour, at which the density gradient was equal to 1–5% of its maximum value inside the shock. It is seen from Fig. 5 that the numerical values deviate from the theoretical polar, beginning from a certain angle of flow deflection $\theta \sim 9$ deg. The maximum angle of flow deflection exceeds its value predicted by the three-shock theory. As can be seen in Fig. 5, the portion of the Mach shock below point A is perfectly described by the incident shock polar: the numerically obtained values of pressure and flow deflection are very close to the incident shock polar. Though the Mach shock angle to the oncoming flow is continuously changing, the shock curvature is negligible, and the flow parameters obey the Rankine–Hugoniot relations. The same applies to the B–C portion of the reflected shock, where the numerically obtained values of pressure and flow deflection are very close to the reflected shock polar. The portion of the reflected shock that is higher than point C lies in the region where the reflected shock is influenced by the expansion waves propagating from the trailing edge of the wedge. The shock intersection region between point A on the Mach shock and point B on the reflected shock is not governed by the Rankine–Hugoniot relations and produces excessive pressure. The flow field between points A and B may be termed as a non-Rankine–Hugoniot zone. This term was introduced in [3] to explain the existence of the irregular shock wave configuration under the von Neumann paradox conditions. As the present study shows, such a viscous transition zone is also observed in reflection of strong shock waves, where the three-shock solution exists.

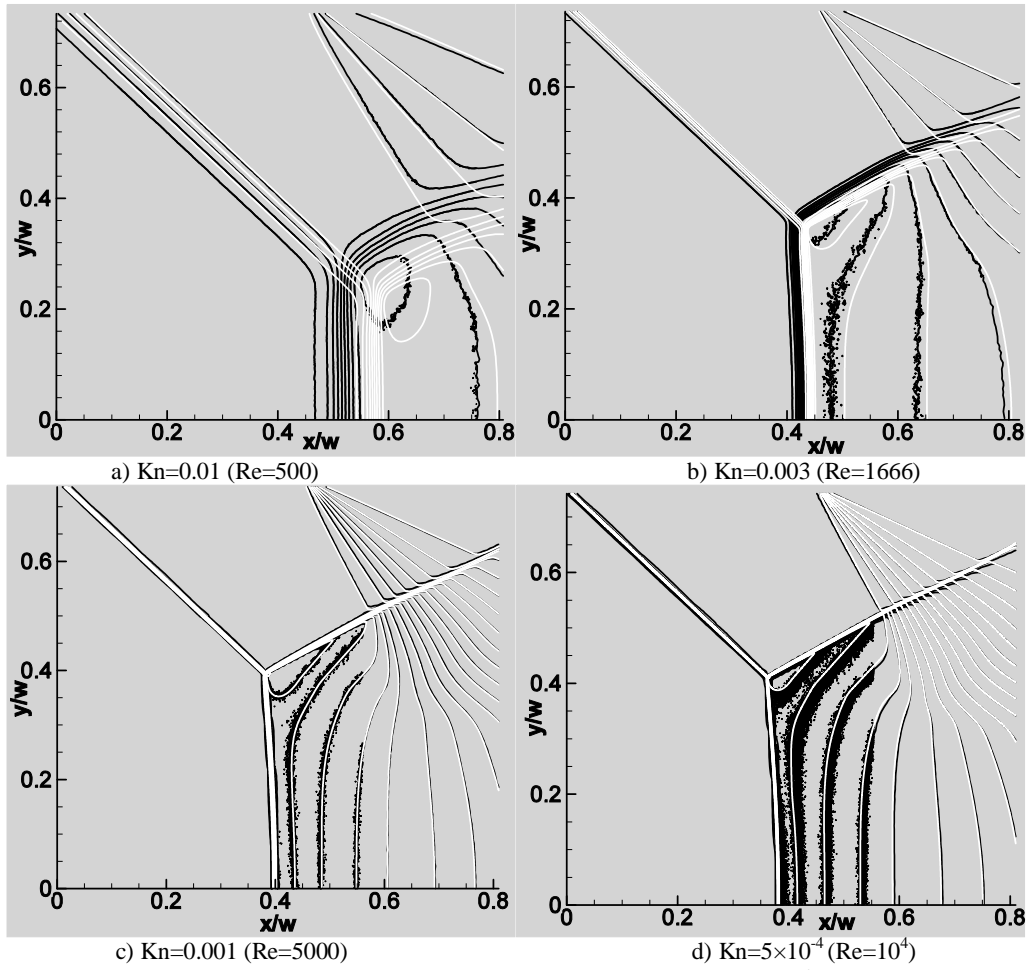


FIGURE 3. Comparison of the pressure contours at different Knudsen numbers. $M_\infty=4$, $\gamma=5/3$, $\Theta_w=25^\circ$. The black and white curves are the results of the DSMC and NS computations, respectively.

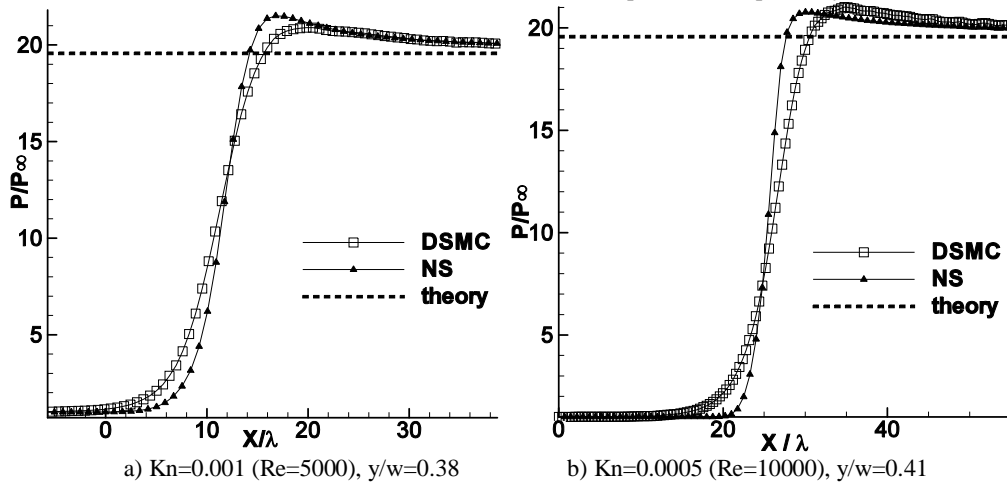


FIGURE 4. Comparison of the pressure profiles at different Knudsen numbers. The dotted curve is the pressure profile predicted by the three-shock theory.

The results of numerical simulations for the von Neumann paradox conditions are shown in Fig. 6a as a comparison of the pressure flow fields of NS and DSMC computations. As in the case of reflection of strong shock waves, the NS and DSMC computations are in good agreement. For a more detailed comparison of the triple-shock structure, Fig. 6b shows the pressure profiles for a constant coordinate $y/w=1.02$. As in the case of reflection of

strong shock waves, differences in the triple-shock profiles are observed. Both the NS and DSMC computations finally converge to one value of pressure.

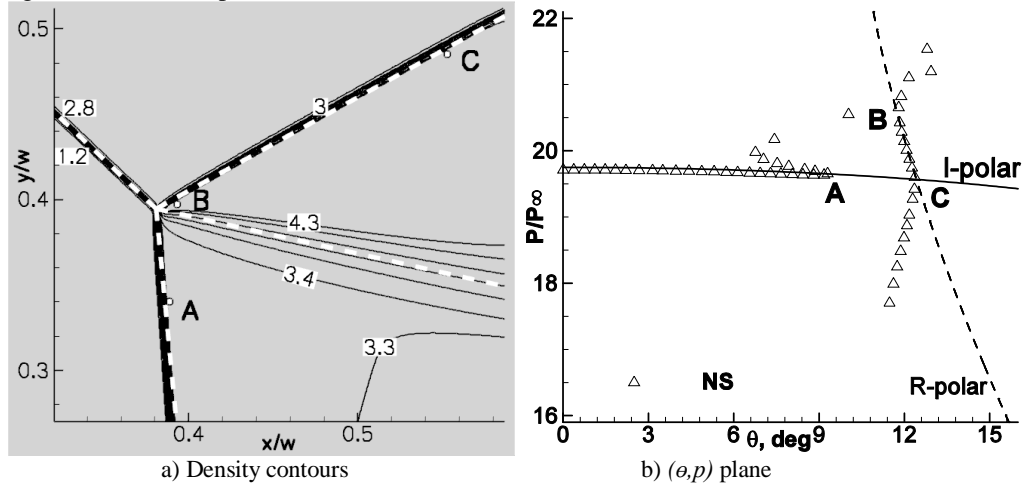


FIGURE 5. Navier–Stokes computation at $M_\infty=4$, $\gamma=5/3$, $\Theta_w=25^\circ$, $Kn=0.001$, $Re=5000$. White dashed curves correspond to theoretical orientations of the shock waves and slipstream.

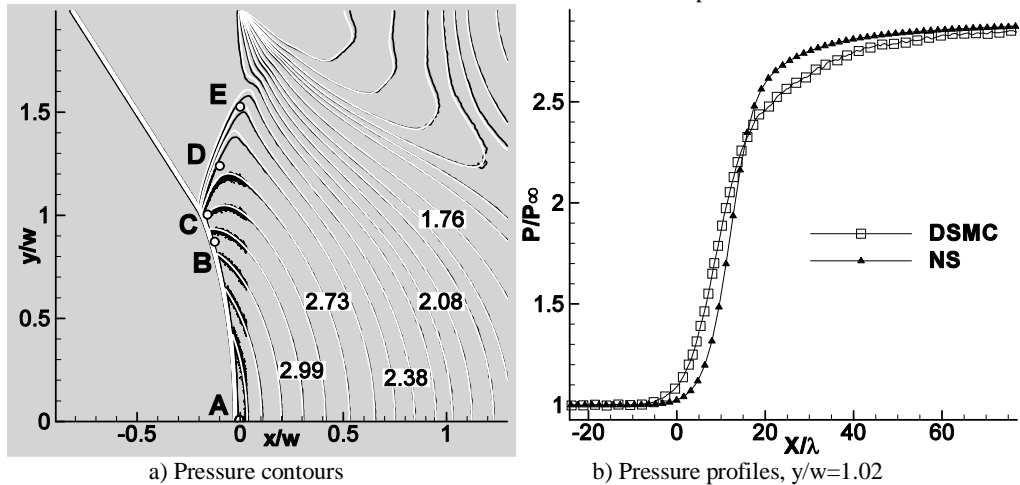


FIGURE 6. Comparison of the NS and DSMC computations. $M_\infty=1.7$, $\gamma=5/3$, $\Theta_w=13.5^\circ$, $Re=2123$, $Kn=0.001$. a) The black and white curves are the results of the DSMC and NS computations, respectively. Points A, B, C, D, and E correspond to the points in the plane (θ, p) in Fig. 7.

The results of our viscous computations are compared with inviscid shock polar solutions in the plane (θ, p) in Fig. 7. It is clearly seen in Fig. 7a that the NS and DSMC computations agree well in the plane (θ, p) . Figure 7b shows a zoomed-in area of the plane (θ, p) , where an isentrope corresponding to the inviscid solution [9,10] is clearly visible. The numerical results in Fig. 7, however, do not coincide with the inviscid solution. We select several characteristic points along the Mach stem and the reflected shock wave. Points A, B, C, D, and E in the plane $(x/w, y/w)$ (in Fig. 6a) correspond to the points in the plane (θ, p) in Fig. 7. Point A is located on the line of symmetry, where the Mach stem is a normal shock wave. Upward along the Mach stem (from point A to point B), the pressure decreases, and the angle of flow deflection increases, which is caused by the curved form of the Mach stem. At point B, the numerical data start to deviate from the theoretical polar. Point C corresponds to the maximum angle of flow deflection. Further motion along the reflected wave leads to a decrease in pressure and the flow deflection angle, with a considerable part of the reflected wave lying outside the reflected wave polar (CD): at a fixed angle of flow deflection, the pressure exceeds the theoretical value. At point D, the numerical data arrive on the reflected wave polar and coincide with the polar up to point E. Starting from point E, the reflected wave starts to interact with the expansion fan emanating from the trailing edge of the wedge. The numerical data pass from the incident wave polar to the reflected wave polar along a curve that does not lie on the polars, i.e., through a zone where viscous effects cause the solution to diverge from the Rankine–Hugoniot conditions. Thus, the existence of such a finite transition zone (BCD) in the viscous case ensures a continuous transition of the gas-dynamic parameters from the incident wave polar to the reflected wave polar. Actually, the BCD zone is a ‘non-Rankine–Hugoniot zone’ [3].

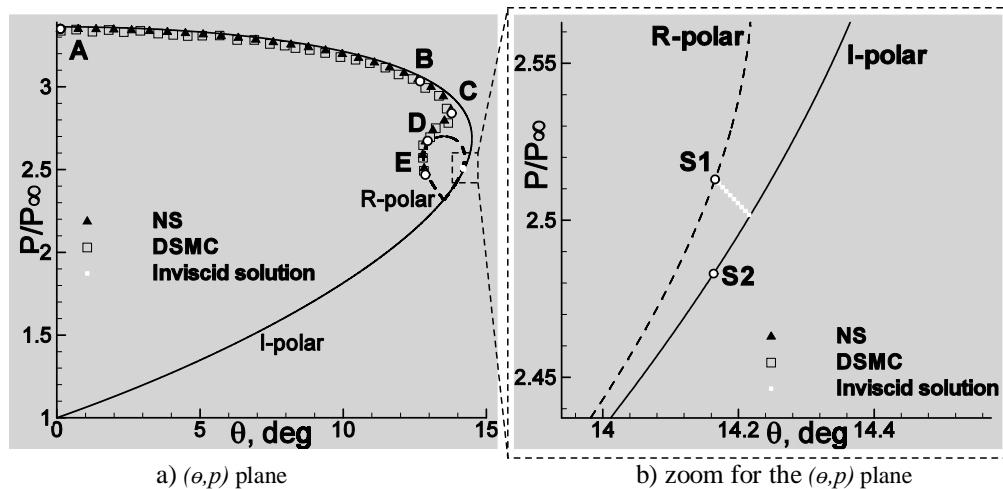


FIGURE 7. Comparison of the NS and DSMC computations in the plane (θ, p) with the inviscid solution. $M_\infty=1.7$, $\gamma=5/3$, $\Theta_w=13.5^\circ$, $Re=2123$, $Kn=0.001$. Points A, B, C, D, and E correspond to the points in the plane $(x/w, y/w)$ in Fig. 6.

CONCLUSION

A steady flow around symmetric wedges with Mach numbers $M_\infty=1.7$ and 4 and Reynolds numbers $Re=500$ –10000 was numerically studied for conditions where the inviscid theory admits the existence of the three-shock solution as well as for conditions where the three-shock solution does not exist (von Neumann paradox conditions). The NS and DSMC computations are in good agreement in both planes $(x/w, y/w)$ and (θ, p) . There is a small difference in the triple-shock structure, which does not affect the behavior of the numerical solution in the plane (θ, p) . Our simulations performed with substantially different approaches suggest that the flow viscosity induces the formation of a smooth three shock transition zone, where one-dimensional Rankine–Hugoniot shock jump relations cannot be applied. The flow parameters in this zone differ from the theoretical values predicted by the inviscid theories.

ACKNOWLEDGMENTS

This work was supported by the by the Russian Foundation for Basic Research (Grant no. 08-01-91307).

REFERENCES

1. M. Ivanov, Ye. Bondar, D. Khotyanovsky, A. Kudryavtsev, G. Shoev, “Viscosity effects on weak irregular reflection of shock waves in steady flow”, *Progress in Aerospace Sciences*, **46**, pp. 89-105 (2010).
2. P. Colella, L. Henderson, “The von Neumann paradox for the diffraction of weak shock waves”, *Fluid Mech.* **213**, pp. 71-94 (1990).
3. J. Sternberg, “Triple-shock-wave intersections”, *Physics of Fluids*, **2**, pp. 179–206 (1959).
4. A. Sakurai, “On the Problem of Weak Mach Reflection”, *Phys Soc Jpn*, **19**, pp. 1440–50 (1964).
5. G. Bird, “Molecular gas dynamics and the direct simulation of gas flows”, Oxford Press, 1994.
6. G. Jiang, C. Shu, “Efficient Implementation of Weighted ENO Schemes”, *J. Comput. Phys.*, **126**, pp. 202–28 (1996).
7. W. Hayes, “The Basic Theory of Gasdynamic Discontinuities”, edited by H. W. Emmons, Princeton Univ. Press, Princeton, 1958.
8. M. Ivanov, G. Markelov, S. Gimelshein, “Statistical simulation of reactive rarefied flows: numerical approach and applications”, *AIAA Paper*, pp. 98-2669, 1998.
9. K. Guderley, “Considerations on the Structure of mixed subsonic–supersonic flow patterns”, HQ Air Materiel Command, Dayton, Ohio, Technical Report F-TR-2168-ND, 1947.
10. E. Vasilev, A. Kraiko, “Numerical simulation of weak shock diffraction over a wedge under the von Neumann paradox conditions”, *Comput Math Phys*, **39**, pp. 1335–45 (1999).